Appl Magn Reson (2014) 45:1253–1260
DOI 10.1007/s00723-014-0597-4

Applied
Magnetic Resonance

Low-Temperature High-Resolution Solid-State (cryoMAS) NMR of Han Purple $BaCuSi_2O_6$

Raivo Stern · Ivo Heinmaa · Enno Joon · Alexander A. Tsirlin · Hiroyuki Nakamura · Tsuyoshi Kimura

Received: 8 August 2014 / Revised: 11 September 2014 / Published online: 30 September 2014

Abstract We present low-temperature (low-T, sub-liquid-N_2) high-speed high-resolution ^{29}Si solid-state (cryoMAS) nuclear magnetic resonance studies on a model 2D-BEC quantum magnet $BaCuSi_2O_6$, known also as Han Purple. We observe broadened ^{29}Si lines below the well-established 100 K structural phase transition confirming the existence of inhomogeneities at low temperatures. Interestingly, the low-T spectra of $BaCuSi_2O_6$ closely resemble those of the novel compound $Ba_2CoSi_2O_6Cl_2$ taken at room temperature. This suggests that the Co compound features structural modulations or inhomogeneities already at room temperature. The low-T crystal structure and magnetism of $BaCuSi_2O_6$ are more complex than previously believed, and deserve further investigation.

1 Introduction

The interest in $BaCuSi_2O_6$ is founded foremost on its extraordinary phase diagram with field-induced Bose–Einstein condensation (BEC) of the excitations (magnons) in an antiferromagnetic (AF) spin system [1, 2]. Being a quantum paramagnet at zero magnetic field down to the lowest temperatures, the system displays a quantum phase transition into a magnetically ordered state at the critical value of the magnetic field of $H_{c1} \sim 23.4\,\mathrm{T}$ [3, 4]. In the layered room-temperature tetragonal crystal structure of $BaCuSi_2O_6$ [5, 6], the copper silicate $Cu_2(SiO_3)_4$ layers are separated by the intermediate layers of Ba atoms (illustration in Fig. 1). Due to the

R. Stern (✉) · I. Heinmaa · E. Joon · A. A. Tsirlin
National Institute of Chemical Physics and Biophysics (NICPB),
Akadeemia tee 23, Tallinn 12618, Estonia
e-mail: raivo.stern@kbfi.ee

H. Nakamura · T. Kimura
Division of Materials Physics, Graduate School of Engineering Science, Osaka University,
Toyonaka, Osaka 560-8531, Japan

staggered location of the Cu_2 dimers with an interatomic distances of ~ 2.75 Å in one layer with respect to the next one, the interdimer Cu − Cu distances are on the one hand quite long (~ 5.75 Å) when going from one copper silicate layer to another, and on the other hand yet larger (~ 7 Å) within a single layer. Thus, the Cu_2 dimers are nearly isolated, and $BaCuSi_2O_6$ is an ideal material prototype of two-dimensionally (2D) arranged weakly coupled spin dimers.

The phenomenon of magnon BEC is essentially the long-range spin order induced by an external magnetic field in an isotropic magnet with SU(2) symmetry [1, 2, 7, 8]. Details of the BEC transition are determined by the interdimer couplings. A unique feature of $BaCuSi_2O_6$ is its 2D-like regime of the BEC in the vicinity of H_{c1} [4]. Most of the theories available on the market [9–13] rely on the idea that the interdimer couplings between the layers are almost perfectly frustrated following the lateral shift of the neighboring layers. This frustration should effectively decouple the layers, thus leading to a 2D-like BEC.

First amendments to this deceptively simple picture were made in 2007 when an inelastic neutron-scattering study of $BaCuSi_2O_6$ revealed two distinct magnetic excitations [14], as opposed to a single excitation, which is expected for identical spin dimers. The ^{63,65}Cu nuclear magnetic resonance (NMR) study simultaneously pinpointed two distinct Cu sites seen below 100 K [15], where $BaCuSi_2O_6$ undergoes a structural phase transition. Details of the low-temperature crystal structure were reported five years later [16]. The transition is of first order and corresponds to the symmetry reduction from tetragonal to orthorhombic, with the

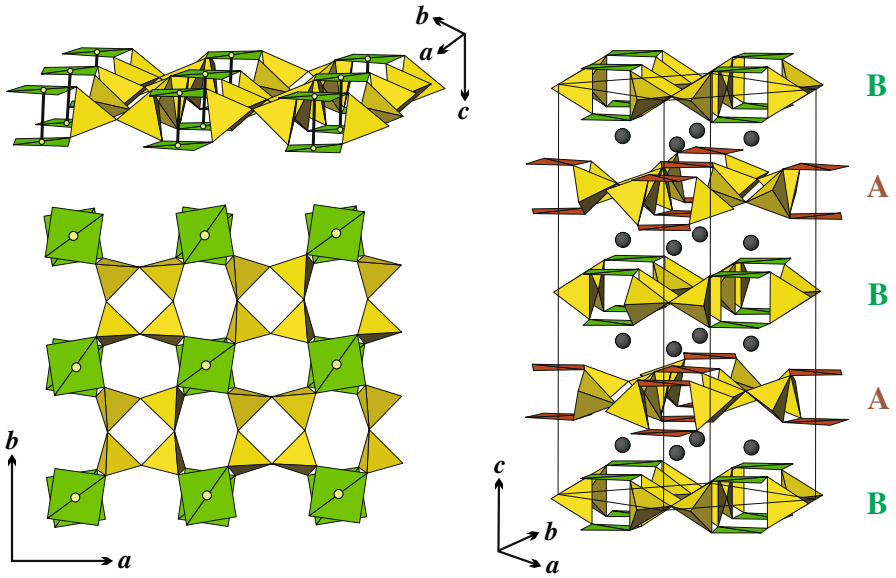

Fig. 1 Crystal structure of $BaCuSi_2O_6$. *Left panel* different projections of a single bilayer of Cu atoms, which is equivalent to one layer of spin dimers. Si atoms are in the *yellow* tetrahedra and coupled to both upper and bottom sites of a dimer. *Right panel* low-temperature orthorhombic crystal structure featuring two types of layers, *A* and *B*, denoted by *brown* and *green colors*, respectively

low-temperature orthorhombic crystal structure featuring two distinct Cu sites within two distinct bilayers that form spin dimers of types A and B (i.e., the dimers with weaker and stronger intradimer couplings, respectively).

Interestingly, a complete microscopic analysis based on the orthorhombic crystal structure [17] challenged one of the key properties of $BaCuSi_2O_6$, the magnetic frustration, because in fact no magnetic frustration—in particular, no frustration of the interlayer couplings—has been found. Earlier theories assumed that the upper site of one dimer is antiferromagnetically coupled to the upper site of the neighboring dimer [14], so that the ordering in the *ab* plane is antiferromagnetic. However, ab initio calculations supported by a re-evaluation of the inelastic neutron-scattering data put forward a different microscopic scenario that entails an upper-to-bottom type of antiferromagnetic interdimer couplings, which then render the ordering in the *ab* plane ferromagnetic. This coupling regime releases the magnetic frustration in $BaCuSi_2O_6$ [17].

The lack of magnetic frustration implies that the magnon BEC in $BaCuSi_2O_6$ should be 3D-like, similar to other spin-dimer systems. Experimentally, this is not the case, though [4]. To resolve this discrepancy, we reconsider the low-temperature crystal structure of $BaCuSi_2O_6$ and address subtle deviations from the orthorhombic structure that might either restore the coveted frustration or give rise to an alternative mechanism of the dimensional reduction of magnon BEC.

NMR on carefully aligned single crystal has been successfully reported for ^{29}Si (and $^{63,65}Cu$) nuclei at low fields as well as in the vicinity of H_{c1} [15, 18, 19], where NMR (and potentially ESR [20]) is still the only spectroscopy applicable around the very high H_{c1} of $BaCuSi_2O_6$. In this static case, the ^{29}Si nucleus senses in addition to the local magnetization of the nearest Cu dimer (via a transferred hyperfine interaction) also direct dipolar interaction. The technique of magic-angle spinning (MAS) is routinely used to reduce linewidths and suppress anisotropic and dipolar interactions in powder samples in a wide range of materials. Recent advances in probe design have extended MAS NMR down to cryogenic temperatures (cryoMAS) and enabled novel insights into various challenging systems: endohedral fullerenes [21–23], fullerides [24], superconductors [25], spin-Peierls materials [26] and even quantum magnets [27]. Here we apply cryoMAS on $BaCuSi_2O_6$ for the first time.

2 Experimental

Polycrystalline samples of $BaCuSi_2O_6$ were prepared by the solid-state reaction. Powders of $BaCO_3$, CuO, and ^{29}Si-enriched SiO_2 were weighed to the prescribed ratios, mixed, and well ground. The mixture was calcined at 900 °C in air for 20 h. The resulting powders were pulverized, and then isostatically pressed into a rod shape (ca 5 mm diameter and 50 mm length) and sintered again at 1,010 °C in air for 20 h.

About 3 mg of finely ground $BaCuSi_2O_6$ powder was packed into a 1.0 mm ZrO_2 rotor. ^{29}Si (spin 1/2) NMR experiments were performed on 8.5 T widebore magnet using an upgraded Bruker AMX 360 console, a helium gas flow cryostat from Janis

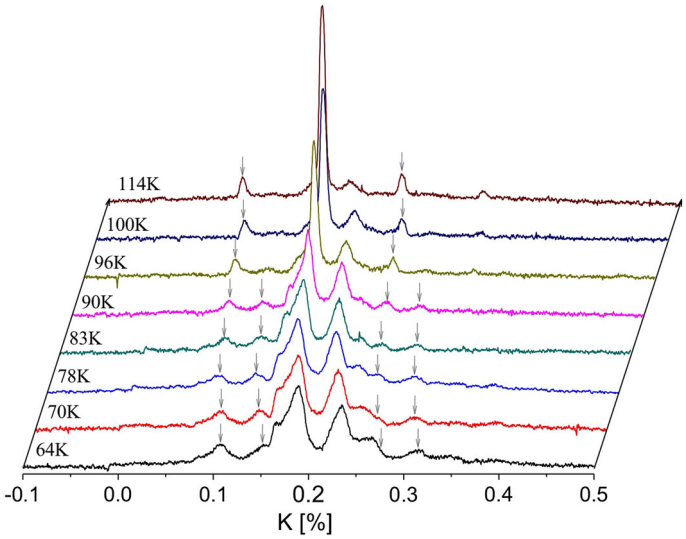

Fig. 2 Temperature dependence of ^{29}Si MAS NMR spectra of $BaCuSi_2O_6$ on heating from 64 to 114 K. The spinning speed of the sample was 60 kHz, each spectrum is the sum of 1,600 averages, relaxation delay 150 ms. Apart from the main lines at isotropic magnetic shift, the spectra show spinning sidebands (denoted by *arrows*) at multiple of the sample spinning speed from the main lines

Research Inc., and a home-built 1.0 mm cryoMAS probe. All spectra are referenced to hexamethyldisiloxane (HMDSO). For the low-T spectra (shown in Fig. 2) the rotor was first cooled with a lower spinning speed of 30–40 kHz down to 40–50 K, then the spinning speed was raised to 65 kHz, and spectra were recorded upon slowly warming the sample from 64 to 114 K. The 64 K spectrum is compared in Fig. 3 with the room-temperature ^{29}Si 15 kHz MAS spectrum recorded in the 4.7 T widebore magnet. For further comparison, a room-temperature ^{29}Si 40 kHz MAS spectrum in 4.7 T of newly discovered $Ba_2CoSi_2O_6Cl_2$ [28] is presented as well (1.8 mm silicon nitride rotor containing 30 mg of powder, natural Si abundance).

3 Results and Discussion

MAS NMR spectra are very sensitive to even smallest structural and magnetic effects. This technique, if applied in a wide enough temperature range, can provide useful information that would otherwise require a single crystal study even on (unoriented) powder. This means that cryoMAS NMR technique can also avoid some potential orientational disorder (mosaicity, twinning, domains) problems with imperfect single crystals. In parallel to those advantages of the cryoMAS technique, it may have serious problems for systems having some magnetic anisotropies (e.g., related to *g*-tensor anisotropy), where MAS spectra would provide just a spatial average, which may eventually smear the phase transitions.

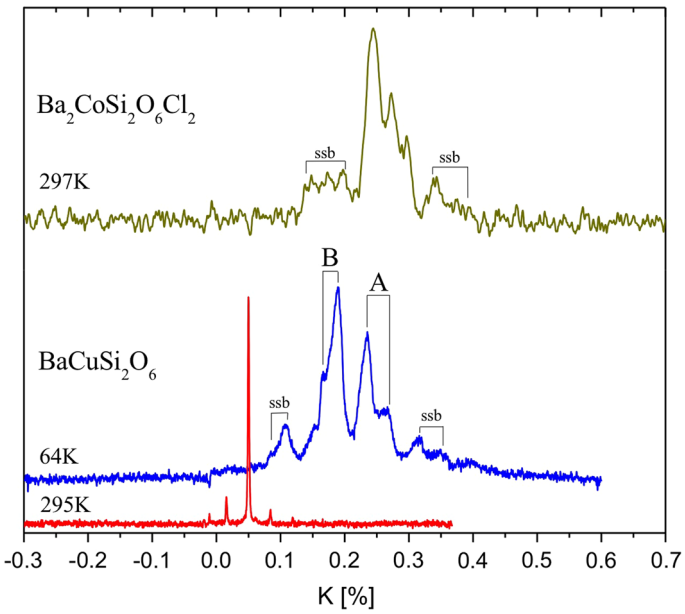

Fig. 3 Comparison of ^{29}Si MAS NMR spectrum of $BaCuSi_2O_6$ at 295 K (*bottom*) to the low temperature spectrum at 64 K and to the spectrum of $Ba_2CoSi_2O_6Cl_2$ at 297 K. The shape of *Line A* and that of *Line B* reflect distribution of magnetic hyperfine field at these sites; *ssb* spinning sidebands (like *arrows* on Fig. 2). The spectrum of $Ba_2CoSi_2O_6Cl_2$ shows broad distribution of the magnetic hyperfine fields already at room temperature

We choose to use ^{29}Si as a probe, because its $I = \frac{1}{2}$ nucleus produces only one spectral line. In $BaCuSi_2O_6$, the single spectral line is indeed seen in the tetragonal phase above 100 K in agreement with the well-established crystallographic data [6]. Below 100 K, we expect at least two lines from the bilayers A and B in the low-temperature orthorhombic crystal structure [16], similarly to the single crystal results for c-axis parallel to the applied field in [15]. We indeed observe two lines that are, however, substantially broadened.

The complex shape of the ^{29}Si NMR line below 100 K indicates the presence of the two groups of strongly distributed local fields. In a magnetic system, the line shift has two components, the chemical shift K_0, which is determined by the local environment of ^{29}Si nuclei and assumed temperature independent, and the magnetic shift, which is a product of the local magnetization on the ^{29}Si nuclei and the hyperfine coupling [15]. From single crystal studies we also know that at 3.1 K, (the lowest temperature of [15]) and even at 40 mK (lowest temperature in high fields of [18]), a single narrow ^{29}Si NMR line is restored. At low temperatures, $BaCuSi_2O_6$ is in the singlet state with the overall magnetization equal to zero. Therefore, we expect that the local magnetization on the Si site is zero as well. Consequently, the contribution of the magnetic shift vanishes, and the remaining single narrow line indicates that all Si atoms in the low-temperature structure of $BaCuSi_2O_6$ have the same chemical shift K_0 within the experimental resolution. In fact, the orthorhombic

Table 1 Estimated shifts (in %), widths (in %), and their ratios from the cryoMAS spectrum at 64 K on Fig. 3

	Center	Inner	Outer	Width	Width/center (%)	J	χ
Line A	0.25	0.23	0.27	0.04	16	50	4.62
Line B	0.18	0.19	0.17	0.02	11	55	4.46

We also provide experimental exchange couplings J (in K) determined from the neutron-scattering study [14], and calculated magnetic susceptibility χ at 64 K (in 10^{-3} emu/mol)

structure of $BaCuSi_2O_6$ features 4 nonequivalent Si sites, but their local environment is so similar (the average Si–O distances are 1.61–1.63 Å [16]) that deviations in the chemical shift should be very small indeed.

For the static sample one source of the broader NMR line could be orientational disorder. Resulting different projections of the anisotropic shift tensor to the applied field direction can contribute to slightly different frequencies and a broad spectral line. In our MAS experiment, such an anisotropy is removed together with the direct dipolar contributions and the observed spread is resulting only from isotropic shifts. Therefore, the line broadening is a direct evidence for the non-uniform local magnetization on the Si nuclei and indicates the presence of a multitude of spin dimers with a spread of intradimer couplings in $BaCuSi_2O_6$ below 100 K. This observation contrasts with only two well-defined couplings J^A and J^B that were derived from the idealized orthorhombic crystal structure [17]. While we do not know the precise origin of this magnetic (and, presumably, structural) inhomogeneity, it is worth noting that a similar effect has been observed in inelastic neutron-scattering experiments [14], where the higher energy dimer excitation B is substantially broadened (Table 1).

From Fig. 2 one can see that the left, low-frequency (smaller magnetization) line continues the extrapolated behavior of the unsplit high-temperature line. Based on the smaller shift, we ascribe this line to dimers B that feature a larger exchange coupling J and, hence, a smaller susceptibility χ. The right, higher-frequency (larger magnetization) line appears a step higher from the high-temperature position. We assign this line to the shorter Cu – Cu and weaker coupled A sites (Fig. 3). Note that this assignment is opposite to Ref. [15], where the larger local magnetization on site B was assumed incorrectly for the ^{29}Si spectra (the ^{63,65}Cu assignment was correct).

$Ba_2CoSi_2O_6Cl_2$ can also be described as an $S = 1/2$ 2D-coupled XXZ dimer model [28], but while in $BaCuSi_2O_6$ structural peculiarities are present already at room temperature, where individual CuO_4 plaquettes are rotated with respect to their ideal positions, the room-temperature structure of $Ba_2CoSi_2O_6Cl_2$ is believed to be free from any distortions. Surprisingly, already the room-temperature ^{29}Si MAS spectrum of $Ba_2CoSi_2O_6Cl_2$ is quite broad. Its shape resembles that of $BaCuSi_2O_6$ at low temperatures, as seen from the direct comparison in Fig. 3. Whether the broad line shape is a fingerprint for the presence of structural distortions also in this novel material, needs to be proved by future studies.

4 Conclusion

We performed the first low-T (sub-liquid-N_2) high-speed high-resolution ^{29}Si solid-state (cryoMAS) NMR studies on a model 2D-BEC quantum magnet $BaCuSi_2O_6$, known also as Han Purple. We observe broadened ^{29}Si lines below the well-established 100 K structural phase transition. The broadened lines pinpoint inhomogeneities of the crystal structure at low temperatures. We note the similarity of the low-T B line to the room-temperature NMR response. The low-T layers look structurally and magnetically similar to the ^{29}Si lines at room temperature of the novel $Ba_2CoSi_2O_6Cl_2$. The complex line shape suggests the presence of the modulations in the latter already at room temperature.

These different pieces of experimental evidence suggest that the low-T crystal structure and magnetism of $BaCuSi_2O_6$ are more complex than previously believed, and their further investigation would be rewarding.

Acknowledgments Work in Tallinn was supported by the Estonian Ministry of Education and Research under Grants SF0690029s09 and SF0690034s09, and by the IUT23-3 and IUT23-7 grants of the Estonian Research Council. IH was supported by the Estonian Science Foundation (ESF) grant ETF8198. AT acknowledges financial support from the ESF via the Mobilitas program (Grant MTT77). RS was funded by the Estonian Research Council (Grants ETF8440 and PUT210). We acknowledge essential discussions with Cristian Batista and Christian Rüegg as well as fruitful communication with Frederic Mila; and all the previous NMR insight by the Grenoble group (Steffen Krämer, Mladen Horvatić, and Claude Berthier). We thank Prof. Hidekazu Tanaka for providing us with the powder of $Ba_2CoSi_2O_6Cl_2$.

References

1. V. Zapf, M. Jaime, C.D. Batista, Rev. Mod. Phys. **86**, 563 (2014)
2. T. Giamarchi, C. Rüegg, O. Tchernyshyov, Nat. Phys. **4**(3), 198 (2008). doi:10.1038/nphys893
3. M. Jaime, V.F. Correa, N. Harrison, C.D. Batista, N. Kawashima, Y. Kazuma, G.A. Jorge, R. Stern, I. Heinmaa, S.A. Zvyagin, Y. Sasago, K. Uchinokura, Phys. Rev. Lett. **93**(8), 087203 (2004)
4. S.E. Sebastian, N. Harrison, C.D. Batista, L. Balicas, M. Jaime, P.A. Sharma, N. Kawashima, I.R. Fisher, Nature **441**(7093), 617 (2006)
5. L.W. Finger, R.M. Hazen, R.J. Hemley, Am. Miner. **74**(7–8), 952 (1989)
6. K.M. Sparta, G. Roth, Acta Crystallogr. Sect. B Struct. Sci. **60**, 491 (2004)
7. Y.M. Bunkov, G.E. Volovik, in *Novel Superfluids*, ed. by K.H. Bennemann, J.B. Ketterson (Oxford University Press, Oxford, 2013).
8. V.M. Kalita, V.M. Loktev, JETP Lett. **91**, 196 (2010)
9. O. Rösch, M. Vojta, Phys. Rev. B **76**(18), 180401 (2007)
10. O. Rösch, M. Vojta, Phys. Rev. B **76**(22), 224408 (2007)
11. C.D. Batista, J. Schmalian, N. Kawashima, P. Sengupta, S.E. Sebastian, N. Harrison, M. Jaime, I.R. Fisher, Phys. Rev. Lett. **98**(25), 257201 (2007)
12. J. Schmalian, C.D. Batista, Phys. Rev. B **77**(9), 094406 (2008)
13. N. Laflorencie, F. Mila, Phys. Rev. Lett. **102**(6), 060602 (2009). doi:10.1103/PhysRevLett.102.060602
14. C. Rüegg, D.F. McMorrow, B. Normand, H.M. Ronnow, S.E. Sebastian, I.R. Fisher, C.D. Batista, S.N. Gvasaliya, C. Niedermayer, J. Stahn, Phys. Rev. Lett. **98**(1), 017202 (2007)
15. S. Krämer, R. Stern, M. Horvatić, C. Berthier, T. Kimura, I.R. Fisher, Phys. Rev. B **76**, 100406 (2007). doi:10.1103/PhysRevB.76.100406
16. D.V. Sheptyakov, V.Y. Pomjakushin, R. Stern, I. Heinmaa, H. Nakamura, T. Kimura, Phys. Rev. B **86**, 014433 (2012)
17. V.V. Mazurenko, M.V. Valentyuk, R. Stern, A.A. Tsirlin, Phys. Rev. Lett. **112**, 107202 (2014)

18. M. Horvatić, C. Berthier, F. Tedoldi, A. Comment, M. Sofin, M. Jansen, R. Stern, Prog. Theor. Phys. Suppl. **159**, 106 (2005)
19. S. Krämer, N. Laflorencie, R. Stern, M. Horvatić, C. Berthier, H. Nakamura, T. Kimura, F. Mila, Phys. Rev. B 87 (2013). doi:10.1103/PhysRevB.87.180405.
20. S.A. Zvyagin, J. Wosnitza, J. Krzystek, R. Stern, M. Jaime, Y. Sasago, K. Uchinokura, Phys. Rev. B **73**(9), 094446 (2006)
21. M. Carravetta, Y. Murata, M. Murata, I. Heinmaa, R. Stern, A. Tontcheva, A. Samoson, Y. Rubin, K. Komatsu, M. Levitt, JACS **126**(13), 4092 (2004). doi:10.1021/ja031536y
22. M. Carravetta, O. Johannessen, M. Levitt, I. Heinmaa, R. Stern, A. Samoson, A. Horsewill, Y. Murata, K. Komatsu, J. Chem. Phys. **124**(10) (2006). doi:10.1063/1.2174012.
23. M. Carravetta, A. Danquigny, S. Mamone, F. Cuda, O.G. Johannessen, I. Heinmaa, K. Panesar, R. Stern, M.C. Grossel, A.J. Horsewill, A. Samoson, M. Murata, Y. Murata, K. Komatsu, M.H. Levitt, Phys. Chem. Chem. Phys. **9**(35), 4879 (2007). doi:10.1039/b707075f
24. A. Potocnik, A.Y. Ganin, Y. Takabayashi, M.T. McDonald, I. Heinmaa, P. Jeglic, R. Stern, M.J. Rosseinsky, K. Prassides, D. Arcon, Chemical Science **5**(8), 3008 (2014). doi:10.1039/c4sc00670d
25. P. Beckett, M.S. Denning, I. Heinmaa, M.C. Dimri, E.A. Young, R. Stern, M. Carravetta, J. Chem. Phys. **137**(11), 114201 (2012). doi:10.1063/1.4751476. http://link.aip.org/link/?JCP/137/114201/1
26. J.M. Law, C. Hoch, R. Glaum, I. Heinmaa, R. Stern, J. Kang, C. Lee, M.H. Whangbo, R.K. Kremer, Phys. Rev. B **83**(18) (2011). doi:10.1103/PhysRevB.83.180414.
27. R. Stern, I. Heinmaa, A. Kriisa, E. Joon, S. Vija, J. Clayhold, M. Ulutagay-Kartin, X. Mo, W. Queen, S. Hwu, Physica B-Condens. Matter **378–380**(1124), 2006 (2005). doi:10.1016/j.physb.2006.01.523 (International Conference on Strongly Correlated Electron Systems (SECES 05), Vienna)
28. H. Tanaka, N. Kurita, M. Okada, E. Kunihiro, Y. Shirata, K. Fujii, H. Uekusa, A. Matsuo, K. Kindo, H. Nojiri, J. Phys. Soc. Jpn. **83**, 103701 (2014). doi:10.7566/JPSJ.83.103701. ArXiv:1404.2033v1